

This discussion paper is/has been under review for the journal *Climate of the Past* (CP).
Please refer to the corresponding final paper in CP if available.

A tropical speleothem record of glacial inception, the South American summer monsoon from 125 to 115 ka

S. J. Burns¹, L. C. Kanner^{1,2}, H. Cheng^{3,4}, and R. L. Edwards⁴

¹Department of Geosciences, University of Massachusetts, Amherst, MA 01003, USA

²Present address: 2nd Nature LLC, 500 Seabright Ave, Santa Cruz, CA 95062, USA

³Institute of Global Environmental Change, Xi'an Jiaotong University, Xi'an 710049, China

⁴Department of Geology and Geophysics, University of Minnesota, Minneapolis, MN 55455, USA

Received: 19 September 2014 – Accepted: 3 October 2014 – Published: 21 November 2014

Correspondence to: S. J. Burns (sburns@geo.umass.edu)

Published by Copernicus Publications on behalf of the European Geosciences Union.

Title Page

Abstract

Introduction

Conclusions

References

Tables

Figures



Back

Close

Full Screen / Esc

Printer-friendly Version

Interactive Discussion



Abstract

Relatively few marine or terrestrial paleoclimate studies have focused on glacial inception, the transition from an interglacial to a glacial climate state. As a result, the timing and structure of glacial inception is not well known, nor is the spatial pattern of glacial inception in different parts of the world. Here we present results of a study of a speleothem from the Peruvian Andes that records changes in the intensity of South American Summer Monsoon (SASM) rainfall over the period from 125 to 115 ka. The results show that late in the last interglacial period, at 123 ka, SASM rainfall decreased, perhaps in response to a decrease in Northern Hemisphere ice cover. Then at 120.8 ka a rapid increase in SASM rainfall marks the end of the last interglacial. After a more gradual increase between 120 and 117 ka, a second abrupt increase occurs at 117 ka. This pattern of change is mirrored to a remarkable degree by changes in the East Asian Monsoon. It is interpreted to reflect both the a long term gradual response of the monsoons the orbitally-driven insolation changes and to rapid changes in Northern Hemisphere ice volume and temperature. Both monsoon systems are close to their full glacial conditions by 117 ka, before any significant decrease in atmospheric CO₂.

1 Introduction

Studies of Earth's transitions from glacial to interglacial states over the past several hundred thousand years have focused on glacial terminations. In particular, the last glacial termination, covering the period from approximately 20–10 ka has been dissected in great detail to better understand how and why glacial conditions yield to a full interglacial (e.g. Cheng et al., 2009a; Denton et al., 2010; Shakun et al., 2012; and references therein). But relatively few paleoclimate studies have focused on the details of the other transition between climate states – glacial inception. The relative age of the most recent glacial inception, about 120 ka, is likely a factor since far fewer

CPD

10, 4365–4384, 2014

SASM glacial inception

S. J. Burns et al.

Title Page

Abstract

Introduction

Conclusions

References

Tables

Figures



Back

Close

Full Screen / Esc

Printer-friendly Version

Interactive Discussion



high resolution archives of climate, either marine or terrestrial, extend so far back in time.

As a result, inferred rates of glacial inception are primarily based on tuning to orbitally driven insolation changes or marine records and are not firmly established by absolutely dated chronologies. Similarly, the timing and pattern of glacial inception in different parts of the world are not well known. Speleothems have often proven useful in adding absolute age chronologies to paleoclimate records, for example, the age and duration of Dansgaard/Oeschger events (Wang et al., 2001; Kanner et al., 2012). They can also yield decadal to sub-decadal resolution paleoclimate information for many regions. Thus well-dated high resolution speleothem records that cover the period of glacial inception have the potential to eliminate uncertainty in the timing and rates of climate change during glacial inception and the relationship between low and high-latitude records. In doing so, they may also help establish the forcing necessary for the transition from one state to another. Here we present a well-dated, high-resolution speleothem record of changes in the South American Summer Monsoon from 125 to 115 ka, a period covering the transition from the penultimate interglacial to the beginning of the last glacial period.

2 Material and methods

Sample P10-H1 is from Huagapo Cave (11.27° S; 75.79° W) ~ 3850 m above sea level (m a.s.l.) in the central Peruvian Andes. The sample is a calcite stalagmite 31.8 cm tall from an upper gallery of the cave approximately 700 m from the main entrance. The sample was cut into halves along the growth axis and polished. For radiometric dating, 10 subsamples were taken about every 30 mm parallel to growth layers. For stable oxygen and carbon isotope analysis, 318 subsamples were taken every millimeter along the growth axis.

The radiometric dates were measured using a multi-collector, inductively coupled plasma mass spectrometry (MC-ICPMS) on a Thermo-Finnigan Neptune at the

**SASM glacial
inception**

S. J. Burns et al.

Title Page

Abstract

Introduction

Conclusions

References

Tables

Figures



Back

Close

Full Screen / Esc

Printer-friendly Version

Interactive Discussion



Minnesota Isotope Laboratory with procedures similar to those described in Cheng et al. (2009b). The stable isotopic analyses were performed at the University of Massachusetts using an on-line carbonate preparation system linked to a Finnigan Delta Plus XL ratio mass spectrometer. Results are reported as the per mil difference between sample and the Vienna Pee Dee Belemnite standard in delta notation where $\delta^{18}\text{O} = (R_{\text{sample}}/R_{\text{standard}} - 1) \cdot 1000$, and R is the ratio of the minor to the major isotope. Reproducibility of the standard materials is better than 0.1‰. Values are reported relative to the VPDB standard.

3 Results

Results of U/Th isotopic analyses (Table 1) show that stalagmite P10-H1 grew from about 125.5 to 115.2 ka. All age determinations are in stratigraphic order and have errors on the order of 0.3%. An age model for the oxygen stable isotope times series was constructed using linear interpolation between each age determination and is shown in Fig. 1.

The oxygen isotope time series is shown in Fig. 2, plotted together with data over the same interval from Hulu Cave in central China (Kelly et al., 2006). The $\delta^{18}\text{O}$ values for P10-H1 range from -12.3 to -17.1 ‰. From 125 to 123 ka the values are centered on -13.5 ‰, then increase to between -12.5 and -13 from 123 to 121 ka. At 120.8 ka, values decrease by more than 1‰ in about 120 years. They continue to decrease more slowly over the next 4 kyr to around -15.5 ‰, show a short-lived, about 75 years in duration, increase of around 0.75‰, then, at 116.8 ka again decrease rapidly to values between -16 and -17 ‰ for the remainder of the record. The second rapid decrease occurs over about 150 years. We note that a cross plot of oxygen vs. carbon stable isotope ratios for P10-H1 has a correlation coefficient (r^2) of 0.06.

4 Discussion

4.1 Interpretation of oxygen isotope variability

The oxygen isotope ratios of speleothem calcite primarily reflect changes in the oxygen isotope ratio of local precipitation (Fairchild et al., 2006; Lachniet, 2009), though factors such as kinetic isotope effects during calcite precipitation, cave temperature, and the isotopic composition of the water vapor source may also be important. We consider these latter three factors first. Kinetic isotope effects are probably present in all speleothems (Daëron et al., 2011), yet kinetic effects can be minimized by sampling at the center of the stalagmite growth axis (Dreybrodt, 2008), which was done here. Another test of whether kinetic effects are important is the “Hendy test” (Hendy, 1971). For sample P10-H1, as noted, carbon and oxygen isotopic values along the growth axis are not correlated ($r^2 = 0.06$), indicating that kinetic effects are not an important influence on oxygen isotope variations.

Figure 2 shows that the least negative $\delta^{18}\text{O}$ values for P10-H1 occur from about 125–121 ka, during the penultimate interglacial period. The most negative values, about 4.8‰ lower, occur at about 115 ka, as earth’s climate made the transition to the long glacial state that followed. Accompanying the transition to a glacial climate, mean annual air temperatures likely decreased by, at most, 5°C at the study site, if we assume that the temperature change was less than or similar to that estimated for the Last Glacial Maximum to Holocene transition (Porter, 2000). Cooler cave temperatures should lead to enriched oxygen isotope ratios in calcite, by about 1‰, due to an increase in the equilibrium calcite-water isotopic fractionation (Kim and O’Neil, 1997). In addition, the transition to a glacial climate resulted in increased global ice volume and an increased oxygen isotope ratio of seawater of around 0.5‰ (using sea level estimates for the time period and a sea level/seawater isotopic ratios of about $0.1\text{‰} \cdot (10\text{ m})^{-1}$). The combined affect of these factors would be to increase the $\delta^{18}\text{O}$ value of speleothem calcite by about 1.5‰. Thus, the observed change of 4.8‰ in

CPD

10, 4365–4384, 2014

SASM glacial inception

S. J. Burns et al.

Title Page

Abstract

Introduction

Conclusions

References

Tables

Figures



Back

Close

Full Screen / Esc

Printer-friendly Version

Interactive Discussion



early Holocene (Kanner et al., 2012, 2013). Thus the SASM was within 80–90 % of its maximum intensity over the last glacial cycle at 116 ka, equivalent to MIS 5.4.

The intensification of the SASM during deglaciation is a response to an increase in summer insolation and an increase in land and sea ice cover at the high northern latitudes both of which influence the mean position of the ITCZ. Numerous paleoclimate studies from the EAM, IM, and SASM regions (Wang et al., 2001, 2005, 2008; Fleitmann et al., 2003; Cruz et al., 2005b) and modeling results (Kutzbach, 1981; Kutzbach et al., 2008; Ziegler et al., 2010) indicate that the primary control on monsoon precipitation is summer insolation changes that follow precession of earth's orbit. The P10-H1 time series follows January insolation at 10° S (Fig. 2), though the response of the SASM to insolation is clearly non-linear. The nadir in SASM intensity and the following increase lag insolation by a few thousand years (Fig. 2). The increase also occurs mainly in two steps, not smoothly. Maximum monsoon intensity, however, is reached at close to the maximum in summer insolation at 10° S.

In addition to insolation, changes in temperature and land and sea ice cover in the high northern latitudes has a strong influence on SASM intensity (Chiang and Bitz, 2005; Broccoli et al., 2006). Paleoclimate studies of speleothem growth periods (Wang et al., 2008) and oxygen isotope ratios (Kanner et al., 2012) during the last glacial period demonstrate that the SASM increased in intensity during Heinrich events and during Greenland stadials. Conversely the SASM was relatively weak during Greenland interstadials. These changes have been interpreted as reflecting millennial-scale shifts in the mean ITCZ position, a hypothesis that is supported by modeling studies of the effect of land and sea ice on the ITCZ and Hadley circulation (Chiang and Bitz, 2005; Broccoli et al., 2006). Similarly, we suggest that the rapid increases in SASM intensity at 121 and 117 ka are due in part to rapid increases in ice cover and decreases in temperature in the high northern latitudes during glacial inception.

CPD

10, 4365–4384, 2014

SASM glacial inception

S. J. Burns et al.

Title Page

Abstract

Introduction

Conclusions

References

Tables

Figures



Back

Close

Full Screen / Esc

Printer-friendly Version

Interactive Discussion



4.2 Comparison to other records

4.2.1 Comparison to changes in East Asian Summer Monsoon

Our record of SASM changes over the transition from MIS 5.5 to 5.4 is mirrored to a remarkable degree by observed changes in the East Asian Monsoon (Fig. 2) as recorded in stalagmites from Dongge Cave in China (Kelly et al., 2006). These records are shown on independent chronologies established by U/Th dating, but with the scale for $\delta^{18}\text{O}$ for Dongge inverted (Fig. 2). During the latter stages of MIS 5.5, the SASM is in a dry phase, while the EASM is in a wet phase. Isotopic values for both speleothems are fairly constant during MIS 5.5, with the exception of a small decrease of about 0.8‰ in $\delta^{18}\text{O}$ values in Huagapo Cave that is mirrored by an increase of about 0.5‰ in Hulu. Both D3 and P10-H1 show a rapid change of more than 2‰ at 120.8 ± 0.5 ka, with a sudden increase in SASM intensity and decrease in EASM intensity. In both records, the majority of this change occurs over less than 200 years. The absolute chronologies of these two tropical speleothems indicate the end of the last interglacial period was associated with a very large, rapid change in tropical hydrology that is synchronous in both hemispheres within the error of the chronologies. The age estimate for rapid climatic change that marks the end of the last interglacial period in Peru and Dongge Cave is also within dating error of speleothems from China, 119 ± 0.6 ka (Yuan et al., 2004), the European Alps 118 ± 2 ka (Meyer et al., 2008) and the Eastern Mediterranean, 119 ± 3 ka (Bar-Matthews et al., 2003). Following this rapid shift is a period of slower change from 121 to 117 during which both isotopic time series parallel their respective summer insolation curves (Fig. 2). A second rapid shift is observed at 117 ka (117.5 in Dongge) with the SASM further strengthening and the EASM further weakening.

SASM glacial inception

S. J. Burns et al.

[Title Page](#)[Abstract](#)[Introduction](#)[Conclusions](#)[References](#)[Tables](#)[Figures](#)[Back](#)[Close](#)[Full Screen / Esc](#)[Printer-friendly Version](#)[Interactive Discussion](#)

4.2.2 Comparison to ice core records

Figure 3 shows the P10-H1 data along with $\delta^{18}\text{O}$ of ice from the NGRIP ice core, $\delta^{18}\text{O}$ of values of atmospheric oxygen from the Vostok ice core and atmospheric methane concentrations from the EPICA dome C core. To incorporate more broadly the P10-H1 data with later changes in the SASM, we spliced data from stalagmite BT2 from Botuvera Cave in southern Brazil (Cruz et al., 2005) to the end of the P10-H1 record. As is the case for P10-H1, the oxygen isotopic values of BT2 are primarily a function of the intensity rainfall in the SASM (Cruz et al., 2005). The growth period of BT2 overlaps growth of P10-H1 for about 2000 years. To put both data sets onto a common $\delta^{18}\text{O}$ scale, 12.5‰ was subtracted from the BT2 values, yielding very similar values for the period of overlap. The BT2 age model was also adjusted for part of the record presented here. Stalagmite BT2 has only four age measurements over the oldest 35 kyr of deposition and the errors for these ages are all greater than 2 % (Cruz et al., 2005). The large isotopic shift at the start of GIS 24 is very well dated in speleothems from Dongge Cave in China (Kelly et al., 2006) and the European Alps (Boch et al., 2011). Therefore, the age of this shift in BT2 was adjusted to 108.0 ka to match the better-dated records. The age adjustment ranges from a maximum of 2700 years at this shift, and decreases to 0 years for ages younger than 102 ka and older than 114 ka. The portion of overlap between BT2 and P10-H1 was not adjusted.

The addition of a record of SASM intensity over the period of glacial inception and the early glacial period leads to the following observations. The GISs 23, 24 and 25 all appear to have a global signal, with increases in atmospheric methane and a decrease in SASM intensity associated with each. Nearly every D/O event found in the ice cores and speleothems is coupled with a parallel change in atmospheric methane (Chappellaz et al., 2013), with Greenland interstadials associated with higher methane concentrations. This relationship is also clearly present in the earliest stages of the glacial period, with GISs 24, 25, and 26 expressed as positive $\delta^{18}\text{O}$ excursions in H09–10b, and increases in methane concentrations in the Vostock and EPICA Dome

SASM glacial inception

S. J. Burns et al.

[Title Page](#)[Abstract](#)[Introduction](#)[Conclusions](#)[References](#)[Tables](#)[Figures](#)[Back](#)[Close](#)[Full Screen / Esc](#)[Printer-friendly Version](#)[Interactive Discussion](#)

**SASM glacial
inception**

S. J. Burns et al.

Title Page

Abstract

Introduction

Conclusions

References

Tables

Figures



Back

Close

Full Screen / Esc

Printer-friendly Version

Interactive Discussion



C ice cores (Fig. 3). By aligning the rapid changes in methane with rapid changes in $\delta^{18}\text{O}$ in the speleothems, a chronology for changes in atmospheric gas concentrations can be established that is independent of age models for the ice cores themselves and independent of the lag in the age of trapped gases with respect to the ice itself.

5 Based on the observed relationship between methane concentrations and millennial-scale events during MIS 3 from speleothems in the region (Kanner et al., 2012), the three methane peaks very likely are coeval with the millennial events in the tropics and with GIS 23, 24 and 25. If so, then either the GT4 chronology for Antarctic ice is a few thousand years too young, or the estimated gas age-ice age difference is too large by
10 a similar amount.

Ice core atmospheric oxygen $\delta^{18}\text{O}$ data from Vostock are also shown in Fig. 3. The $\delta^{18}\text{O}_{\text{atm}}$ values are reach a first minimum in following MIS 5.5 that is coincident with the first minimum in atmospheric methane, which the speleothem chronologies place at 116 ka, just at the transition from GS25 to GIS25 (Landais et al., 2006). We show
15 the EDC methane record because it is higher resolution than Vostok methane, note that both are on the same timescale. The large change in tropical hydrology associated with this decrease supports the hypothesis that on millennial timescales $\delta^{18}\text{O}_{\text{atm}}$ responds strongly to changes in the monsoons (Bender et al., 1994; Hoffmann et al., 2004). It is also worth noting that in the EPICA Dome C ice core, CO_2 concentrations remain
20 above 260 ppmv through the entire observed decrease in methane from 130 ka to 113 ka (GT4 timescale, or ~ 115 ka using the stalagmite timescale). Thus, CO_2 remains above 260 ppmv during the entire period of NH cooling and ice growth through the first minimum in stalagmite P10-H1 in Peru and maximum in stalagmite D3 in China. These results are in accord with modeling studies that suggest that orbital forcing alone is
25 sufficient to result in the growth of ice sheets in the Northern Hemisphere.

The timing of glacial inception recorded in the speleothems in both hemispheres, however, is considerably earlier, and therefore under conditions of relatively high summer insolation, than is usually used in modeling studies. Modeling results indicate that tropical hydrology responds very rapidly to ice sheet expansion (Chiang and Bitz,

2005; Broccoli et al., 2006) Thus it is reasonable to infer from the speleothem $\delta^{18}\text{O}$ records that rapid ice sheet growth began as early as 120 ka, at approximately the mid-point in the insolation curve for NH summer insolation.

4.3 Implications for sea-level reconstructions

5 The speleothem $\delta^{18}\text{O}$ data and the accuracy of the dating of the curves, also have implications for the timing of sea-level changes thought to have taken place during MIS 5.5 and at the 5.5–5.4 transition. A number of studies have concluded that there was a rapid sea-level rise near the end of MIS 5.5 (O’Leary et al., 2013; Dutton and Lambeck, 2012; Thompson et al., 2011). This rise is thought to have been the results of a rapid melting event in the high Northern latitudes. If so, it is likely that this event would have impacted tropical hydrology, just as millennial scale events did during glacial periods. We observe a nearly 1 per mille increase in speleothem $\delta^{18}\text{O}$ in our Huagapo Cave record at 123 ka, coincident with an ~ 0.5 per mille decrease in the Hulu cave record (Kelly et al., 2006). These data suggest a significant weakening in the SASM and strengthening of the EASM, as models predict for a warming of the high N latitudes and decrease in ice cover there. We suggest that the abrupt change in tropical hydrology is associated with the late MIS 5.5 sea-level change observed in other archives.

15 A related question is the timing of ice accumulation and sea-level fall at the end of MIS 5.5. The speleothem records indicate that the end of MIS 5.5 in the tropics, marked by a rapid weakening of the EASM and strengthening of the SASM, occurred at 120.8 ± 0.4 ka (dating errors on P10–01 are less than 400 years, those for speleothems D3 and D4 from Hulu are ~ 1000 years). We infer that these changes in the monsoon are a direct response to high northern latitude cooling and increasing ice cover. In contrast, coral records of the timing of the end of MIS 5.5 indicate that sea-level remained at or above present sea-level until 115–117 ka (O’Leary et al., 2013; Dutton and Lambeck, 2012; Thompson et al., 2011). While it is not possible to make a direct

Title Page

Abstract

Introduction

Conclusions

References

Tables

Figures



Back

Close

Full Screen / Esc

Printer-friendly Version

Interactive Discussion



SASM glacial inception

S. J. Burns et al.

Title Page

Abstract

Introduction

Conclusions

References

Tables

Figures



Back

Close

Full Screen / Esc

Printer-friendly Version

Interactive Discussion



estimate of sea-level fall from the speleothem records, it is unlikely that the very large changes in tropical hydrology observed could have taken place without at least several meters of sea-level equivalent ice growth. Thus, we suggest that the coral ages used to estimate the timing of sea-level fall are several thousand years too young, and are more impacted by diagenesis and the uncertainty in seawater $\delta^{234}\text{U}$ than is commonly recognized.

5 Conclusions

A speleothem recovered from Huagapo cave in the Peruvian Andes records variations in the intensity of South American Summer Monsoon rainfall in the Amazon Basin from 125–114 ka, covering the transition from the penultimate interglacial period to the following glacial period. SASM rainfall was relatively low during the latter part of MIS 5.5, but increased rapidly at 120.8 ka as rapidly decreasing temperatures and increasing ice cover in the high northern latitudes, marking the beginning of the last glacial period, pushed the mean position of the ITCZ to the south. By 116.8 ka the SASM intensity was as high as at any point during the entire last glacial period. Both the timing and pattern of changes in the SASM are mirrored to a high degree of fidelity by anti-phase changes in the East Asian Summer Monsoon. The timing of these changes in tropical hydrology thus reveals the nature of the interglacial to glacial transition at low latitudes. A full tropical “glacial” state was reached before any decrease in atmospheric CO_2 , suggesting that insolation forcing alone is sufficient to terminate interglacial periods.

References

Andersen, K. K. and North Greenland Ice Core Project members: High-resolution record of Northern Hemisphere climate extending into the last interglacial period, *Nature*, 431, 147–151, 2004.

SASM glacial inception

S. J. Burns et al.

Title Page

Abstract

Introduction

Conclusions

References

Tables

Figures



Back

Close

Full Screen / Esc

Printer-friendly Version

Interactive Discussion



- Bar-Matthews, M., Ayalon, A., Gilmour, M., Matthews, A., and Hawkesworth, C.: Sea–land oxygen isotopic relationships from planktonic foraminifera and speleothems in the Eastern Mediterranean region and their implication for paleorainfall during interglacial intervals, *Geochim. Cosmochim. Ac.*, 67, 3181–3199, 2003.
- 5 Bender, M., Sowers, T., and Labeyrie, L.: The Dole Effect and its variations during the last 130 000 years as measured in the Vostok Ice Core, *Global Biogeochem. Cy.*, 8, 363–376, 1994.
- Berger, A.: Long-term variations of daily insolation and quaternary climatic changes, *J. Atmos. Sci.*, 35, 2362–2367, 1978.
- 10 Boch, R., Cheng, H., Spötl, C., Edwards, R. L., Wang, X., and Häuselmann, P.: NALPS: a precisely dated European climate record 120–60 ka, *Clim. Past*, 7, 1247–1259, doi:10.5194/cp-7-1247-2011, 2011.
- Broccoli, A. J., Dahl, K. A., and Stouffer, R. J.: Response of the ITCZ to Northern Hemisphere cooling, *Geophys. Res. Lett.*, 33, L01702, doi:10.1029/2005GL024546, 2006.
- 15 Chappellaz, J., Stowasser, C., Blunier, T., Baslev-Clausen, D., Brook, E. J., Dallmayr, R., Fain, X., Lee, J. E., Mitchell, L. E., Pascual, O., Romanini, D., Rosen, J., and Schüpbach, S.: High-resolution glacial and deglacial record of atmospheric methane by continuous-flow and laser spectrometer analysis along the NEEM ice core, *Clim. Past*, 9, 2579–2593, doi:10.5194/cp-9-2579-2013, 2013.
- 20 Cheng, H., Edwards, R. L., Broecker, W. S., Denton, G. H., Kong, X., Wang, Y., Zhang, R., and Wang, X.: Ice age terminations, *Science*, 326, 248–252, 2009a.
- Cheng, H., Fleitmann, D., Edwards, R. L., Wang, X., Cruz, F. W., Auler, A. S., Mangini, A., Wang, Y., Kong, X., Burns, S. J., and Matter, A.: Timing and structure of the 8.2 kyr B.P. event inferred from $\delta^{18}\text{O}$ records of stalagmites from China, Oman, and Brazil, *Geology*, 37, 1007–1010, 2009b.
- 25 Chiang, J. C. H. and Bitz, C. M.: Influence of high latitude ice cover on the marine Intertropical Convergence Zone, *Clim. Dynam.*, 25, 477–496, 2005.
- Cruz, F. W., Burns, S. J., Karmann, I., Sharp, W. D., Vuille, M., Cardoso, A. O., Ferrari, J. A., Dias, P. L. S., and Viana, O.: Insolation-driven changes in atmospheric circulation over the past 116 000 years in subtropical Brazil, *Nature*, 434, 63–66, 2005.
- 30 Daëron, M., Guo, W., Eiler, J., Genty, D., Blamart, D., Boch, R., Drysdale, R., Maire, R., Wainer, K., and Zanchetta, G.: $^{13}\text{C}^{18}\text{O}$ clumping in speleothems: observations from natural caves and precipitation experiments, *Geochim. Cosmochim. Ac.*, 75, 3303–3317, 2011.

SASM glacial inception

S. J. Burns et al.

Title Page

Abstract

Introduction

Conclusions

References

Tables

Figures



Back

Close

Full Screen / Esc

Printer-friendly Version

Interactive Discussion



- Denton, G. H., Anderson, R. F., Toggweiler, J. R., Edwards, R. L., Schaefer, J. M., and Putnam, A. E.: The last glacial termination, *Science*, 328, 1652–1656, 2010.
- Dreybrodt, W.: Evolution of the isotopic composition of carbon and oxygen in a calcite precipitating $\text{H}_2\text{O}-\text{CO}_2-\text{CaCO}_3$ solution and the related isotopic composition of calcite in stalagmites, *Geochim. Cosmochim. Ac.*, 72, 4712–4724, 2008.
- Dutton, A. and Lambeck, K.: Ice volume and sea level during the last interglacial, *Science*, 337, 216–219, 2012.
- Fairchild, I., Smith, C., Baker, A., Fuller, L., Spotl, C., Matthey, D., and McDermott, F.: EIMP: modification and preservation of environmental signals in speleothems, *Earth-Sci. Rev.*, 75, 105–153, 2006.
- Fleitmann, D., Burns, S. J., Mudelsee, M., Neff, U., Kramers, J., Mangini, A., and Matter, A.: Holocene forcing of the Indian monsoon recorded in a stalagmite from Southern Oman, *Science*, 300, 1737–1739, 2003.
- Garreaud, R., Vuille, M., and Clement, A. C.: The climate of the Altiplano: observed current conditions and mechanisms of past changes, *Palaeogeogr. Palaeoclimatol.*, 194, 5–22, 2003.
- Hendy, C.: The isotopic geochemistry of speleothems – I. The calculation of the effects of different modes of formation on the isotopic composition of speleothems and their applicability as palaeoclimatic indicators, *Geochim. Cosmochim. Ac.*, 35, 801–824, 1971.
- Hoffmann, G., Cuntz, M., Weber, C., Ciais, P., Friedlingstein, P., Heimann, M., Jouzel, J., Kaduk, J., Maier-Reimer, E., Seibt, U., and Six, K.: A model of the Earth's Dole effect, *Global Biogeochem. Cy.*, 18, GB1008, doi:10.1029/2003GB002059, 2004.
- Kanner, L. C., Burns, S. J., Cheng, H., and Edwards, R. L.: High-latitude forcing of the South American summer monsoon during the last glacial, *Science*, 335, 570–573, 2012.
- Kanner, L. C., Burns, S. J., Cheng, H., Edwards, R. L., and Vuille, M.: High-resolution variability of the South American summer monsoon over the last seven millennia: insights from a speleothem record from the central Peruvian Andes, *Quaternary Sci. Rev.*, 75, 1–10, 2013.
- Kelly, M. J., Edwards, R. L., Cheng, H., Yuan, D., Cai, Y., Zhang, M., Lin, Y., and An, Z.: High resolution characterization of the Asian Monsoon between 146 000 and 99 000 years BP from Dongge Cave, China and global correlation of events surrounding Termination II, *Palaeogeogr. Palaeoclimatol.*, 236, 20–38, 2006.
- Kim, S.-T. and O'Neil, J. R.: Equilibrium and nonequilibrium oxygen isotope effects in synthetic carbonates, *Geochim. Cosmochim. Ac.*, 61, 3461–3475, 1997.

**SASM glacial
inception**

S. J. Burns et al.

Title Page

Abstract

Introduction

Conclusions

References

Tables

Figures



Back

Close

Full Screen / Esc

Printer-friendly Version

Interactive Discussion



- Kutzbach, J. E.: Monsoon climate of the early Holocene: climate experiment with the earth's orbital parameters for 9000 years ago, *Science*, 214, 59–61, 1981.
- Kutzbach, J. E., Liu, X., Liu, Z., and Chen, G.: Simulation of the evolutionary response of global summer monsoons to orbital forcing over the past 280 000 years, *Clim. Dynam.*, 30, 567–579, 2008.
- Lachniet, M. S.: Climatic and environmental controls on speleothem oxygen-isotope values, *Quaternary Sci. Rev.*, 28, 412–432, 2009.
- Landais, A., Masson-Delmotte, V., Jouzel, J., Raynaud, D., Johnsen, S., Huber, C., Leuenberger, M., Schwander, J., and Minster, B.: The glacial inception as recorded in the NorthGRIP Greenland ice core: timing, structure and associated abrupt temperature changes, *Clim. Dynam.*, 26, 273–284, 2006.
- Meyer, M. C., Spötl, C., and Mangini, A.: The demise of the Last Interglacial recorded in isotopically dated speleothems from the Alps, *Quaternary Sci. Rev.*, 27, 476–496, 2008.
- O'Leary, M. J., Hearty, P. J., Thompson, W. G., Raymo, M. E., Mitrovica, J. X., and Webster, J. M.: Ice sheet collapse following a prolonged period of stable sea level during the last interglacial, *Nat. Geosci.*, 6, 796–800, 2013.
- Petit, J. R., Jouzel, J., Raynaud, D., Barkov, N. I., Barnola, J.-M., Basile, I., Bender, M., Chappellaz, J., Davis, M., Delaygue, G., Delmotte, M., Kotlyakov, V. M., Legrand, M., Lipenkov, V. Y., Lorius, C., Pépin, L., Ritz, C., Saltzman, E., and Stievenard, M.: Climate and atmospheric history of the past 420 000 years from the Vostok ice core, Antarctica, *Nature*, 399, 429–436, 1999.
- Porter, S. C.: Snowline depression in the tropics during the Last Glaciation, *Quaternary Sci. Rev.*, 20, 1067–1091, 2000.
- Seltzer, G., Rodbell, D., and Burns, S.: Isotopic evidence for late Quaternary climatic change in tropical South America, *Geology*, 28, 35–38, 2000.
- Shakun, J. D., Clark, P. U., He, F., Marcott, S. A., Mix, A. C., Liu, Z., Otto-Bliesner, B., Schmittner, A., and Bard, E.: Global warming preceded by increasing carbon dioxide concentrations during the last deglaciation, *Nature*, 484, 49–54, 2012.
- Spahni, R., Chappellaz, J., Stocker, T. F., Loulergue, L., Hausammann, G., Kawamura, K., Flückiger, J., Schwander, J., Raynaud, D., Masson-Delmotte, V., and Jouzel, J.: Atmospheric methane and nitrous oxide of the late Pleistocene from Antarctic ice cores, *Science*, 310, 1317–1321, 2005.

**SASM glacial
inception**

S. J. Burns et al.

[Title Page](#)[Abstract](#)[Introduction](#)[Conclusions](#)[References](#)[Tables](#)[Figures](#)[Back](#)[Close](#)[Full Screen / Esc](#)[Printer-friendly Version](#)[Interactive Discussion](#)

- Thompson, W. G., Allen Curran, H., Wilson, M. A., and White, B.: Sea-level oscillations during the last interglacial highstand recorded by Bahamas corals, *Nat. Geosci.*, 4, 684–687, 2011.
- Vimeux, F., Gallaire, R., Bony, S., Hoffmann, G., and Chiang, J. C. H.: What are the climate controls on δD in precipitation in the Zongo Valley (Bolivia)? Implications for the Illimani ice core interpretation, *Earth Planet. Sc. Lett.*, 240, 205–220, 2005.
- 5 Vuille, M. and Werner, M.: Stable isotopes in precipitation recording South American summer monsoon and ENSO variability: observations and model results, *Clim. Dynam.*, 25, 401–413, 2005.
- Wang, Y., Cheng, H., Edwards, R. L., He, Y., Kong, X., An, Z., Wu, J., Kelly, M. J., Dykoski, C. A., and Li, X.: The Holocene Asian monsoon: links to solar changes and North Atlantic climate, *Science*, 308, 854–857, 2005.
- 10 Wang, Y., Cheng, H., Edwards, R. L., Kong, X., Shao, X., Chen, S., Wu, J., Jiang, X., Wang, X., and An, Z.: Millennial-and orbital-scale changes in the East Asian monsoon over the past 224 000 years, *Nature*, 451, 1090–1093, 2008.
- 15 Wang, Y. J., Cheng, H., Edwards, R. L., An, Z. S., Wu, J. Y., Shen, C. C., and Dorale, J. A.: A high-resolution absolute-dated late Pleistocene monsoon record from Hulu Cave, China, *Science*, 294, 2345–2348, 2001.
- Yuan, D., Cheng, H., Edwards, R., Dykoski, C., Kelly, M., Zhang, M., Qing, J., Lin, Y., Wang, Y., Wu, J., Dorale, J., An, Z., and Cai, Y.: Timing, duration, and transitions of the Last Interglacial Asian Monsoon, *Science*, 304, 575–578, 2004.
- 20 Ziegler, M., Lourens, L. J., Tuenter, E., Hilgen, F., Reichert, G.-J., and Weber, N.: Precession phasing offset between Indian summer monsoon and Arabian Sea productivity linked to changes in Atlantic overturning circulation, *Paleoceanography*, 25, PA3213, doi:10.1029/2009PA001884, 2010.

SASM glacial
inception

S. J. Burns et al.

Table 1. ^{230}Th dating results P10-H1.

Sample depth (mm)	^{238}U (ppb)	^{232}Th (ppt)	$^{230}\text{Th} / ^{232}\text{Th}$ (atomic $\times 10^{-6}$)	$d^{234}\text{U}^a$ (measured)	$^{230}\text{Th} / ^{238}\text{U}$ (activity)	^{230}Th Age (years) (uncorrected)	^{230}Th Age (years) (corrected)	$d^{234}\text{U}_{\text{initial}}^b$ (corrected)	^{230}Th Age (yr BP) ^c (corrected)	
11	338.8 ± 0.5	1529 ± 31	13890.2 ± 278	4189.4 ± 5.8	3.8023	0.0068	115 696 ± 373	115 677 ± 373	5806.6 ± 10	115 617 ± 373
45	407.4 ± 0.4	1242 ± 25	19793.7 ± 397	3958.2 ± 3.7	3.6593	0.0058	117 197 ± 314	117 125 ± 314	5258 ± 11	117 065 ± 314
80	50.6 ± 0.1	128 ± 3	25 978 ± 522	4351.9 ± 4.2	3.9865	0.0056	118 503 ± 294	118 493 ± 294	6080 ± 8	118 433 ± 294
105	612.5 ± 0.7	48 ± 2	828 184 ± 26 136	4324 ± 4	3.9716	0.0060	118 803 ± 305	118 802 ± 424	6046 ± 7	118 740 ± 424
144	404.5 ± 0.5	1658 ± 33	15 959 ± 320	4306 ± 5	3.9679	0.0060	119 264 ± 325	119 247 ± 325	6029 ± 9	119 187 ± 325
194	487.2 ± 0.6	2128 ± 43	14 944 ± 300	4260.8 ± 4.3	3.9600	0.0057	120 519 ± 311	120 500 ± 311	5987 ± 8	120 440 ± 311
212	416.1 ± 0.5	1139 ± 23	24 631 ± 495	4368 ± 4	4.0887	0.0061	122 641 ± 320	121 629 ± 442	6175 ± 8	121 567 ± 442
231	676.0 ± 0.8	7134 ± 143	6391 ± 128	4366.4 ± 4.1	4.0908	0.0059	122 811 ± 314	122 769 ± 316	6174 ± 8	122 709 ± 316
253	491.7 ± 0.6	7723 ± 155	4372 ± 88	4420.1 ± 4.5	4.1651	0.0060	124 317 ± 328	124 254 ± 330	6277 ± 9	124 194 ± 330
290	509 ± 1	789 ± 16	45 053.9 ± 908	4487.8 ± 4.7	4.2334	0.0075	125 006 ± 390	124 999 ± 390	6386 ± 10	124 939 ± 390

The error is 2s error. ^a $\delta^{234}\text{U} = ((^{234}\text{U}/^{238}\text{U})_{\text{activity}} - 1) \times 1000$.

^b $\delta^{234}\text{U}_{\text{initial}}$ was calculated based on ^{230}Th age (T), i.e., $\delta^{234}\text{U}_{\text{initial}} = \delta^{234}\text{U}_{\text{measured}} \times e^{1234 \times T}$.

Corrected ^{230}Th ages assume the initial $^{230}\text{Th}/^{232}\text{Th}$ atomic ratio of $4.4 \pm 2.2 \times 10^{-6}$. Those are the values for a material at secular equilibrium, with the bulk earth $^{232}\text{Th}/^{238}\text{U}$ value of 3.8. The errors are arbitrarily assumed to be 50%.

^c BP stands for "Before Present" where the "Present" is defined as the year AD 1950.

Title Page

Abstract

Introduction

Conclusions

References

Tables

Figures



Back

Close

Full Screen / Esc

Printer-friendly Version

Interactive Discussion



**SASM glacial
inception**

S. J. Burns et al.

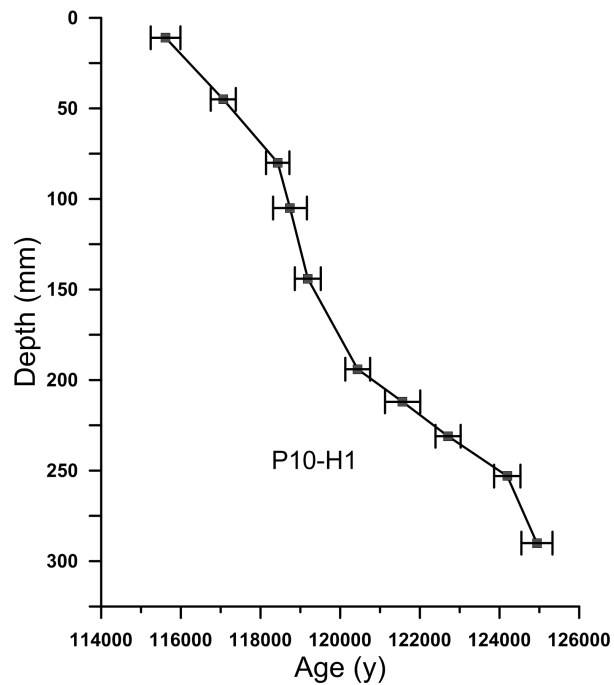


Figure 1. Age vs. depth for stalagmite P10-H1. Error bars are 2 sigma.

[Title Page](#)[Abstract](#)[Introduction](#)[Conclusions](#)[References](#)[Tables](#)[Figures](#)[◀](#)[▶](#)[◀](#)[▶](#)[Back](#)[Close](#)[Full Screen / Esc](#)[Printer-friendly Version](#)[Interactive Discussion](#)

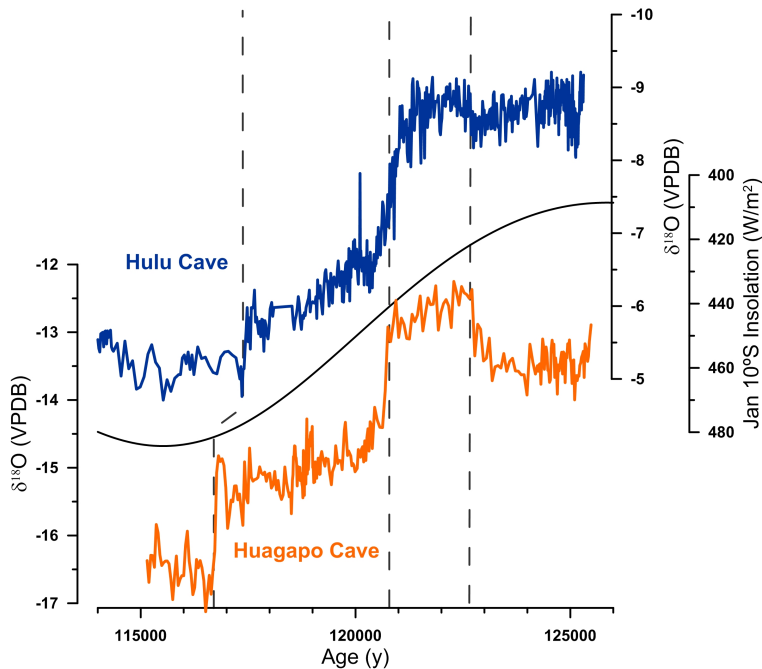


Figure 2. $\delta^{18}\text{O}$ values for P10-H1 from Huagapo Cave in Peru plotted together with $\delta^{18}\text{O}$ values for stalagmites from Hulu Cave in China (Kelly et al., 2006) and the insolation curve for 10°S in January (Berger, 1978).

SASM glacial inception

S. J. Burns et al.

[Title Page](#)

[Abstract](#) | [Introduction](#)

[Conclusions](#) | [References](#)

[Tables](#) | [Figures](#)

[◀](#) | [▶](#)

[◀](#) | [▶](#)

[Back](#) | [Close](#)

[Full Screen / Esc](#)

[Printer-friendly Version](#)

[Interactive Discussion](#)



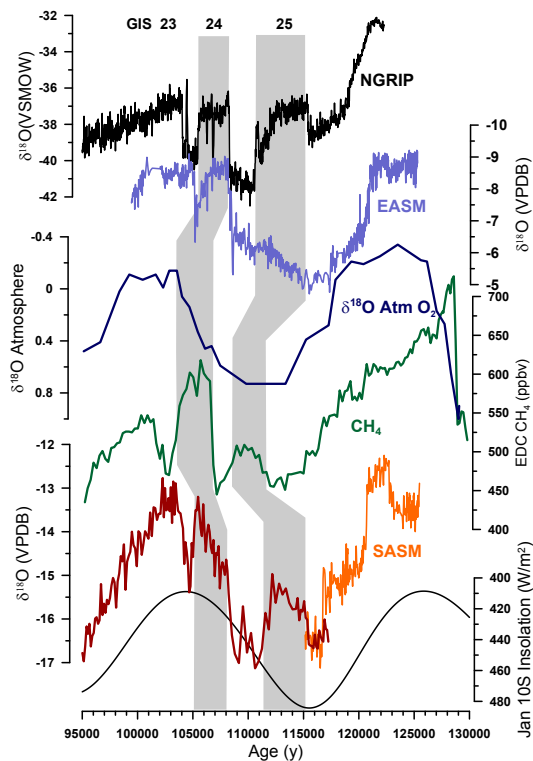


Figure 3. Oxygen isotope proxies for changes in the intensity of the South American Summer Monsoon, SASM (Cruz et al., 2005 and this paper), East Asian Monsoon, EASM (Kelly et al., 2006) and Greenland temperatures, NGRIP (Andersen et al., 2004), atmospheric methane concentrations from the Epica Dome C ice core (Spahni et al., 2005) and $\delta^{18}\text{O}$ values for atmospheric oxygen from the Vostok ice core (Petit et al., 1999). The records are all on independent timescales.

Title Page

Abstract

Introduction

Conclusions

References

Tables

Figures



Back

Close

Full Screen / Esc

Printer-friendly Version

Interactive Discussion

